Journal of Materials Science

Structure, Viscosity and Fibre Drawing Properties of Phosphate Based Glasses: Effect of Boron and Iron Oxide Addition

--Manuscript Draft--

Manuscript Number:	JMSC-D-16-00642R2
Full Title:	Structure, Viscosity and Fibre Drawing Properties of Phosphate Based Glasses: Effect of Boron and Iron Oxide Addition
Article Type:	Manuscript (Regular Article)
Keywords:	Keywords: Phosphate based glasses, phosphate glass fibres, thermal stability, FTIR, viscosity, fragility parameter.
Corresponding Author:	Nusrat Sharmin, Ph. D University of Nottingham Ningbo China Ningbo, CHINA
Corresponding Author Secondary Information:	
Corresponding Author's Institution:	University of Nottingham Ningbo China
Corresponding Author's Secondary Institution:	
First Author:	Nusrat Sharmin, Ph. D
First Author Secondary Information:	
Order of Authors:	Nusrat Sharmin, Ph. D
	Ifty Ahmed, PhD
	Andy Parsons, PhD
	Chris Rudd, PhD
Order of Authors Secondary Information:	
Abstract:	ABSTRACT Resorbable phosphate based glasses have been applied as fibrous reinforcement for resorbable polymers for fracture fixation. The mechanical properties of these composites largely depend on the mechanical properties of the fibres. In this current study, four phosphate based glass compositions were produced by replacing Na2O with B2O3 and/or Fe2O3 in the glass system P2O5-CaO-Na2O-MgO, and the P2O5 content was fixed at 45 mol%. The thermal stability of the glasses containing both B2O3 and Fe2O3 and/or FeO (P45B5Fe5 and P45B5Fe3) was significantly higher than the only B2O3 (P45B5) or Fe2O3 (P45Fe3 and P45Fe5) containing glasses. The viscosity was found to shift to higher temperature with increasing B2O3 and Fe2O3 and/or FeO content. The fragility parameter, m and F1/2, estimated from the viscosity curve, decreases with B2O3 addition. The improved physical properties of the glasses investigated with B2O3 and Fe2O3 and/or FeO addition were attributed to the replacement of P-O-P bonds with P-O-B and P-O-Fe bonds. The presence of P-O-B and P-O-Fe bonds in the glass structure was confirmed by the FTIR analysis. It was possible to draw continuous fibres up to 3 hours from the B2O3 or Fe2O3 and/or FeO containing glasses, whereas it was difficult to pull fibre from only Fe2O3 containing glasses and the fibre pulling process was not continuous. Therefore, addition of B2O3 to the glass system enabled successful drawing of continuous fibres from glasses with phosphate (P2O5) contents of 45 mol%. It was also observed that addition of only Fe2O3 and/or FeO did not have a significant effect on the fibre mechanical properties, whilst the mechanical properties of the fibres increased with increasing B2O3.
Funding Information:	

February 1, 2016

Editor in Chief
Journal of Materials Science

Dear Sir/ Madam,

We are submitting our manuscript, "Structure, viscosity and fibre drawing properties of phosphate based glasses: Effect of boron and Iron oxide addition" for publication as an original research article in the Journal of Materials Science.

The main aim of this study was to investigate the mechanical properties of these composites largely depend on the mechanical properties of the fibres. In this current study, four phosphate based glass compositions were produced by replacing Na_2O with B_2O_3 and/or Fe_2O_3 in the glass system P_2O_5-CaO-Na_2O-MgO, and the P_2O_5 content was fixed at 45 mol%. The thermal stability of the glasses containing both B_2O_3 and Fe_2O_3 and/or FeO (P45B5Fe5 and P45B5Fe3) was significantly higher than the only B_2O_3 (P45B5) or Fe_2O_3 (P45Fe3 and P45Fe5) containing glasses. The viscosity was found to shift to higher temperature with increasing B_2O_3 and Fe_2O_3 and/or FeO content. The fragility parameter, *m* and $F_{1/2}$, estimated from the viscosity curve, decreases with B_2O_3 addition. The improved physical properties of the glasses investigated with B_2O_3 and Fe_2O_3 and/or FeO addition were attributed to the replacement of P-O-P bonds with P-O-B and P-O-Fe bonds. The presence of P-O-B and P-O-Fe bonds in the glass structure was confirmed by the FTIR analysis. It was possible to draw continuous fibres up to 3 hours from the B_2O_3 or Fe_2O_3 and/or FeO containing glasses, whereas it was difficult to pull fibre from only Fe_2O_3 containing glasses and the fibre pulling process was not continuous. Therefore, addition of B_2O_3 to the glass system enabled successful drawing of continuous fibres from glasses with phosphate (P_2O_5) contents of 45 mol%. It was also observed that addition of only Fe_2O_3 and/or FeO did not have a significant effect on the fibre mechanical properties, whilst the mechanical properties of the fibres increased with increasing B_2O_3.
We confirm that this manuscript has not been published elsewhere and is not under consideration by another journal. All authors have approved the manuscript and agree with submission to the journal of Materials Science. The authors have no conflicts of interest to declare.

Reviewers Name:

Jonathan Knowles (e-mail: jonathan.knowles@ucl.ac.uk)
Ruhul Amin Khan (e-mail: rakhan@mech.ubc.ca)
Delia Brauer (e-mail: delia.brauer@uni-jena.de)

Please address all correspondence to

Nusrat Sharmin
Department of Chemical and Environmental Engineering
Faculty of Science and Engineering
University of Nottingham Ningbo, China
Tel:+86(0)57488189242
e-mail: Nusrat_sharmin27@yahoo.com; Nusrat.Sharmin@nottingham.edu.cn

Journal of Materials Science - Decision on Manuscript Number- JMSC-D-16-00642

Title: Structure, Viscosity and Fibre Drawing Properties of Phosphate Based Glasses: Effect of Boron and Iron Oxide Addition

**Responses to the authors are shown using Italic letter and blue font.*

Editor(s)' Comments to Author:

Comments to the Author

Figure 1 contains machine-generated text (i.e., at the bottom of the micrographs). This needs to be removed before we can accept this paper for publication.

Response: The machine-generated text at the end Figure has been removed.

Structure, Viscosity and Fibre Drawing Properties of Phosphate Based Glasses: Effect of Boron and Iron Oxide Addition

Nusrat Sharmin[a,b,c*], Chris D. Rudd[b,c], Andrew J. Parsons[d] and Ifty Ahmed[e]

[a]*Department of Chemical and Environmental Engineering, Faculty of Science and Engineering, University of Nottingham Ningbo China, Ningbo 315100, China*

[b]*Ningbo Nottingham International Academy for the Marine Economy and Technology, University of Nottingham Ningbo China, 315100, China*

[c]*Ningbo Nottingham New Materials Institute, University of Nottingham Ningbo China, Ningbo 315100, China*

[d]*Composites Research Group, Healthcare Technologies, Faculty of Engineering, University of Nottingham, NG7 2RD, UK*

[e]*Advanced Materials Research Group, Healthcare Technologies, Faculty of Engineering, University of Nottingham, NG7 2RD, UK*

*Corresponding authors. Present address: Room 339, Science and Engineering Building, Faculty of Science and Engineering, University of Nottingham Ningbo, 199 Taikang East Rd, Ningbo 315100, China. Tel: +86057488189242

E-mail address: Nusrat.Sharmin@nottingham.edu.cn; nusrat_sharmin27@yahoo.com

ABSTRACT

Resorbable phosphate based glasses have been applied as fibrous reinforcement for resorbable polymers for fracture fixation. The mechanical properties of these composites largely depend on the mechanical properties of the fibres. In this current study, four phosphate based glass compositions were produced by replacing Na_2O with B_2O_3 and/or Fe_2O_3 in the glass system P_2O_5-CaO-Na_2O-MgO, and the P_2O_5 content was fixed at 45 mol%. The thermal stability of the glasses containing both B_2O_3 and Fe_2O_3 and/or FeO (P45B5Fe5 and P45B5Fe3) was significantly higher than the only B_2O_3 (P45B5) or Fe_2O_3 (P45Fe3 and P45Fe5) containing glasses. The viscosity was found to shift to higher temperature with increasing B_2O_3 and Fe_2O_3 and/or FeO content. The fragility parameter, *m* and $F_{1/2}$, estimated from the viscosity curve, decreases with B_2O_3 addition. The improved physical properties of the glasses investigated with B_2O_3 and Fe_2O_3 and/or FeO addition were attributed to the replacement of P-O-P bonds with P-O-B and P-O-Fe bonds. The presence of P-O-B and P-O-Fe bonds in the glass structure was confirmed by the FTIR analysis. It was possible to draw continuous fibres up to 3 hours from the B_2O_3 or Fe_2O_3 and/or FeO containing glasses, whereas it was difficult to pull fibre from only Fe_2O_3 containing glasses and the fibre pulling process was not continuous. Therefore, addition of B_2O_3 to the glass system enabled successful drawing of continuous fibres from glasses with phosphate (P_2O_5) contents of 45 mol%. It was also observed that addition of only Fe_2O_3 and/or FeO did not have a significant effect on the fibre mechanical properties, whilst the mechanical properties of the fibres increased with increasing B_2O_3.

Keywords: Phosphate based glasses, phosphate glass fibres, thermal stability, FTIR, viscosity, fragility parameter.

INTRODUCTION

Phosphate based glasses without silica and with high CaO/P_2O_5 molar ratio have a great potential to be used for biomedical applications as their chemical composition is close to that of natural bone. However, a very high temperature is required to prepare these glasses and often have the tendency to crystallise [1]. Therefore, different modifier oxides have been added to PBGs to improve the thermal stability and durability of the glasses to suit the end application. Phosphate based glasses (PBGs) have the property of being completely soluble in aqueous medium and their degradation rate can easily be altered via addition of different modifier oxides. These unique physical and chemical properties of PBGs have attracted huge interest in their use within the field of biomaterials and tissue engineering [2-5].

In recent years, iron phosphate glasses have received increasing attention because of their high thermal stability, chemical durability, high compositional flexibility and low melting points. These characteristics of iron phosphate glasses have prompted substantial research in the past decade aimed at utilising them as hosts for the immobilisation of toxic and nuclear wastes [6-8]. More recently, there has been a growing interest in using the iron phosphate glasses for different biomedical applications [9, 10]. However, a number of studies have shown that the iron phosphate glasses tend to crystallise at relatively low temperatures, which is a common problem associated with the drawing of PBG fibres [8], as they would tend to crystallise at the working process temperature [11], particularly with Q^0 and Q^1 dominated structures. Mössabauer spectroscopy revealed that iron can be present as both Fe^{2+} and Fe^{3+} in iron phosphate glasses and the concentration of Fe^{2+} decreased with increasing Fe_2O_3 content [8].

B_2O_3 is known to improve the thermal stability of PBGs by suppressing their tendency to crystallise by altering the dimensionality of the phosphate network via the formation of long chain Q^2 species rather than smaller Q^0 or Q^1 units [1, 12, 13]. Moreover, it has been reported that the addition of 5 and 10 mol% of B_2O_3 to the phosphate glasses increased the thermal stability by reducing the tendency to crystallise [14].With this in mind, it was hypothesised that the addition of B_2O_3 content in the iron phosphate glass formulation could improve the thermal properties of the glasses by forming long chain structures.

The addition of B_2O_3 to PBGs has been reported to significantly improve the thermal stability and durability of the glass systems [14]. It has also been reported that the addition of B_2O_3 made the fibre production a continuous process with greater ease [15, 16]. Therefore, the aim

of the current study was to investigate the effect of B_2O_3 addition on the thermal, structure, viscosity and fibre drawing properties of PBG glasses in the system P_2O_5-CaO-MgO-Na_2O-Fe_2O_3 with phosphate contents fixed at 45 mol%. The main reason for attempting to achieve this was that previous studies from the group had shown a much more favourable cytocompatible response for PBG formulations containing Fe_2O_3, however proved very difficult to fiberise. The results from this study showed that continuous fibres from PBG formulations with P_2O_5 contents of 45mol% could be fiberised continuously without breaking with addition of B_2O_3. In addition, the effect of B_2O_3 and/or Fe_2O_3 addition on the mechanical properties of the as drawn fibres was also evaluated.

MATERIALS AND METHODOLOGY

Glass preparation

Four different glass compositions were prepared (see Table 1) using sodium dihydrogen phosphate (NaH_2PO_4, Sigma Aldrich, UK, ≥ 99%), calcium hydrogen phosphate ($CaHPO_4$, Sigma Aldrich, UK, 98-105%), magnesium hydrogen phosphate trihydrate ($MgHPO_4.3H_2O$) , boron oxide (B_2O_3, Sigma Aldrich, UK, ≥99%), iron (III)-phosphate dehydrate ($FePO_4.2H_2O$, Sigma Aldrich, UK, ≥26%) and phosphorous pentoxide (P_2O_5, Sigma Aldrich, UK, >98%) (Sigma Aldrich, UK) as starting materials. The precursors were mixed together and around 120gm of precursors were transferred to a 200 ml volume Pt/5% Au crucible (Birmingham Metal Company, U.K.), which was then placed in a furnace (preheated to 350 ^oC) for half an hour for the removal of H_2O. The salt mixtures were then melted in a furnace at 1150 ^oC for 1.5 hours. Molten glass was poured onto a steel plate, left to cool and then ground into powder using a pestle and mortar.

Compositional analysis

Compositional analysis was conducted using inductively coupled plasma atomic emission spectroscopy (ICP-AES, Perkin Elmer Optima 7300, MA, USA) (see Table 2). Before each cycle of measurement, calibration curves were obtained by preparing standard solutions containing B, P, Na^+, Ca^{2+}, Fe^{3+} and Mg^{2+} (Perkin Elmer, USA) at concentrations of 1, 10 and 100 ppm in 2% HNO_3 in DI water. Standard sample concentrations were measured periodically to ensure accuracy of the calibration curves. ICP-AES analyses for each extract was performed in triplicate (n=3 extracts per variable). For analysis 0.1g of each formulation was digested in 5 ml 70% HCl until a clear solution was obtained. The solution was then diluted 100 times using 2% HNO_3 in DI water prior to ICP-AES analysis.

Thermal Analysis

Glass pieces of the various compositions were ground to fine powder using a pestle and mortar. The glass transition temperature (T_g) of the glasses was determined using differential scanning calorimeter (DSC, TA Instruments Q10, UK). A sample of each glass composition was heated from room temperature to 520 ^oC at a rate of 20 $^oC\ min^{--1}$ in flowing argon gas. The T_g was extrapolated from the onset of change in the endothermic reaction of the heat flow [17].

To determine the onset of crystallisation a different DSC instrument (TA Instruments SDT Q600, UK) was used. Samples were heated from room temperature to a value of T_g+20 ^oC at a rate of 20 $^oC\ min^{-1}$, held there isothermally for 15 min and then cooled down at a rate of 10 $^oC\ min^{-1}$ to 40 ^oC before ramping up again to 1100^oC a rate of 20 $^oC\ min^{-1}$ under flowing argon gas. The samples were subjected to the programmed heating cycle to introduce a known thermal history. A blank run was carried out to determine the baseline which was then subtracted from the traces obtained. The T_g was determined from the second ramping cycle in the same process discussed above. The first deviation of the DSC curve from the baseline above T_g before crystallisation peak was taken as the onset of crystallisation temperature. The Thermal stability of the glasses was measured in terms of the processing window by taking the temperature interval between T_g and the onset of crystallisation temperature ($T_{c,ons}$) as shown in Equation 1 below.

$$\text{Processing Window} = T_{c,ons} - T_g \qquad \text{Equation 1}$$

Fourier transform infrared (FTIR) spectroscopic analysis

Infrared spectroscopy was performed on a Bruker Tensor-27 spectrometer (Germany). All spectra were analysed using Opus^{TM} software version 5.5. The glass samples were crushed and ground into fine powder using a mineral mortar and pestle. The samples were scanned in absorbance mode in the region of 4000 to 550 cm^{-1} (wave numbers) using standard Pike attenuated total reflectance (ATR) cell (Pike technology, UK).

Viscosity/temperature measurements

A parallel plate method was used for viscosity (η)/temperature measurements in the range of 8 Pa s < log (η) < 5.5 Pa s using a thermo-mechanical analyser (Perkin Elmer

Thermomechanical Analyser TMA 7). For this process small glass rods with diameters of approximately 4 mm and average heights of 3 mm were used. The samples were sandwiched between two stainless steel plates, where the top plate was fitted to the TMA silica sample probe. A force of 170 mN was applied to the top plate via the sample probe. During the experiments helium gas was passed through the sample chamber at 20 ml min^{-1}. During the process the temperature was increased initially from room temperature to T_g at 40°C min^{-1}, kept isothermally at T_g for 3 minutes and then increased again to T_g+120°C at 5°C min^{-1}. Gent's [18] equation was employed to obtain the viscosity/temperature behaviour of the glass forming liquids investigated. The equation is:

$$\eta = \frac{\mathbf{2\,\pi F h^5}}{\mathbf{3V\,(\,2\pi h^3 + V)\,(dh/dt)}} \qquad \text{Equation 2}$$

where, F is the applied force, h is the sample height at time t and V is the sample volume.

At high temperatures a rotational viscometer was used (Brookfield DV-III UTRA, USA). The viscosity was measured by measuring the force required to rotate a spindle in the molten glass. The viscosity was determined by measuring the shear stress and the shear rate exerted by the viscous fluid on a rotating cylindrical platinum spindle according to:

$$\eta = \frac{\tau}{\dot{\gamma}} \qquad \text{Equation 3}$$

where, η is the viscosity in poise, $\dot{\gamma}$ is the rate of shear in sec^{-1} and τ is the shear stress in dynes/cm^2. Calibration was undertaken by use of the borosilicate glass standard reference material 717a which has been described by Parsons et al. [19].

In order to derive a viscosity curve for each of the nine glasses, the data points from both the parallel plate method and rotational method were combined and fitted to the Fulcher equation by a least squares calculation [20]. The equation is:

$$\mathrm{Log}_{10}\,\eta = \mathrm{A} + \frac{\boldsymbol{B}}{\boldsymbol{T - T_o}} \qquad \text{Equation 4}$$

where, T is the temperature in °C, η is the viscosity in Pa s and A, B and T_o are constants. The values of the constants/parameters calculated for each of the samples are given in Table 4.

Fragility is a qualitative concept which addresses the deviations of liquid relaxation times from Arrhenius behaviour [21]. In order to compare the viscosity/temperature behaviour of

different glass super cooled melts Angell [22] introduced kinetic fragility of liquids expressed by dimensionless a steepness index m at the glass transition temperature which can be defined as:

$$m = \left. \frac{d\,(\log_{10}\eta)}{d\,(T_g/T)} \right|_{T=T_g} \qquad \text{Equation 5}$$

Figure 5 represents the plot of log η versus T_g/T which shows the variable bending according to the strength of the melt, where, T_g was obtained by running DSC scans at 10°C/ min scanning rate. The slope of the plot at T_g provides the fragility index (m). Alternatively, using VFT parameters,

$$m = B.T_g.\,(T_g - T_o)^{-2} \qquad \text{Equation 6}$$

An alternative fragility index ($F_{1/2}$) has also been introduced as [23]:

$$F_{1/2} = 2\,(T_g/T_{1/2} - 0.5) \qquad \text{Equation 7}$$

where $T_{1/2}$ is the temperature when the viscosity is halfway (log η=3.5) (on logarithmic scale) between log η=12 (characteristics of the glass transition temperature for non-fragile liquids) and log η=-5 (which is the roughly common high-temperature limiting value) [23]. The values of m and $F_{1/2}$ calculated for each of the samples are given in Table 5.

Fibre drawing process

Continuous fibres approximately ~20 μm diameter were produced via a melt-draw spinning process using a dedicated in-house facility. Figure 1 shows the SEM images of the as drawn fibres. The pulling temperature was adjusted to around 1150°C. The molten glass was pushed though the bushing by hydrostatic pressure and was collected on a rotating drum.

Single fibre filament test

Single fibre filament tests (SFTT) were conducted in accordance with ISO 11566 [24]. Twenty fibres were mounted individually onto plastic tabs for each sample, with a 25mm gauge length testing setup. The ends of each fibre were bonded to the plastic tab with an acrylic adhesive (Dymax 3099 - Dymax, Europe) and the adhesive was cured using UV light. In order to determine the individual diameter of each fibre prior to testing, the fibre specimens were measured by using a laser scan micrometer, LSM 6200 (Mitutoyo, Japan).

The laser scan micrometer was calibrated with glass fibre of known diameters (determined by SEM) and the error on diameter measurements is considered to be ±0.3 μm. The SFTT was performed using a LEX810 Tensile Tester (UK) at room temperature with a load capacity of 0.2 N and a speed of 0.017 mm s^{-1}. The student's t-test was used to study the effect of composition on the tensile fracture stress and modulus values of the fibres. Significance was detected at a 0.05 level and all statistical analysis was carried out using GraphPad Prism for Windows (GraphPad, Software Inc, USA).

The Weibull distribution is a well-known and accepted method to describe the strength of fibres [25]. Weibull modulus and normalising stress are found statistically as the shape and scale factors. The normalising stress σ_o can be regarded as the most probable stress at which a fibre of length *Lo* will fail. PBG fibres are essentially brittle and Weibull distribution is an accepted statistical tool used to characterize the failure mode of brittle fibres. In this study, Weibull parameters were obtained from the tensile fracture stress data calculated using Minitab® 15 (version 3.2.1).

RESULTS

Thermal Analysis

Table 3 shows the effect of B_2O_3 (5 mol%) and Fe_2O_3 (3 and 5 mol%) addition on the T_g of the glasses in the systems of $45P_2O_5$-16CaO-24MgO-(15-x)Na_2O-3Fe_2O_3-xB_2O_3 and $45P_2O_5$-16CaO-24MgO-(15-x)Na_2O-3Fe_2O_3- xB_2O_3 (where x=0 and 5). The T_g values increased with increasing Fe_2O_3 content from 3 to 5 mol%. An increase in T_g was also observed with B_2O_3 (5 mol%) addition. The T_g values increased from 470°C to 485°C as the Fe_2O_3 content was increased from 3 to 5 mol%. However, the T_g values increased to 502°C and 513°C as 5 mol% B_2O_3 was added to the P45Fe3 and P45Fe5 glass systems, respectively.

The values for the processing window ($T_{c,ons}$ -T_g), which is also an indication of the thermal stability for glasses, are presented in Figure 2**.** The values for the processing window were seen to increase as B_2O_3 was added to the P45Fe3 and P45Fe5 glass systems. With 5 mol% B_2O_3 addition, the processing window increased from 72°C to 77 °C and 71 °C to 80 °C for P45Fe3 and P45Fe5 glass formulations, respectively.

Fourier transform infrared (FTIR) spectroscopy

The structural properties of the glasses as a function of B_2O_3 content were investigated using infrared spectroscopy. The IR spectra of glasses can be seen in Figure 3. The four bands in the IR spectra of only Fe_2O_3 containing glasses (P45Fe3 and P45Fe5) were observed at 730 cm^{-1}, 908 cm^{-1}, 1097 cm^{-1} and 1245 cm^{-1}. It was observed that the intensity of the band detected at 730 cm^{-1} of the P45Fe3 and P45Fe5 glasses decreased and shifted to the higher wave number (742 cm^{-1}) as B_2O_3 was added to the glass systems. A similar variation was observed for the band at 908 cm^{-1}. The band shifted to the higher wave number (920 cm^{-1}) and the intensity of the band also decreased as 5 mol% B_2O_3 was added to P45Fe3 and P45Fe5 glass systems. The intensity of the bands at 1097 cm^{-1} and 1245 cm^{-1} were also seen to decrease with B_2O_3 addition. However, this time the bands shifted to a lower wave number.

Viscosity/ temperature analysis

Figure 4 shows the measured Log η as a function of temperature. At high temperature, the viscosities of the glass forming liquids containing boron were greater than those with no boron. However, there appeared to be a convergence between P45Fe3 and P45Fe5; P45B5Fe3 and P45B5Fe5 at lower temperature.

A fragility plot was constructed in which the reciprocal temperature was normalised to T_g obtained from running DSC scans at 10 ^oC/min heating rate (see Figure 5). The fragility indices *m* and $F_{1/2}$ were calculated according to equations 6 and 7, respectively. It was observed that both the $F_{1/2}$ and m values followed the same trend and were seen to decrease as 5 mol% B_2O_3 was added to the P45Fe3 and P45Fe5 glass formulations. However, an increase in fragility index was observed when the Fe_2O_3 content was increased from 3 to 5 mol% for both set of glass forming liquids. The $F_{1/2}$ values of P45Fe3 and P45Fe5 glass forming liquids are 0.63 and 0.64, whilst the $F_{1/2}$ values decreased to 0.60 and 0.61 for P45B5Fe3 and P45B5Fe5 glasses, respectively. The m values of P45Fe3 and P45Fe5 were found to decrease to 29 and 31 as 5 mol% B_2O_3 was added to the glass systems.

Mechanical properties of as-drawn fibres

Figure 6 shows the mechanical properties (tensile strength and modulus) of the fibres produced from the glass system $45P_2O_5$-16CaO-24MgO-(12-x)Na_2O-$3Fe_2O_3$-xB_2O_3 and $45P_2O_5$-16CaO-24MgO-(10-x)Na_2O-$5Fe_2O_3$- xB_2O_3 (where x=0 and 5). An increase in tensile strength was seen as 5 mol% B_2O_3 was added to the P45Fe3 and F45Fe5 glasses. Whereas, no significant difference ($P > 0.05$) in tensile strength was observed as Fe_2O_3 content alone was increased from 3 to 5 mol%. The tensile strengths of P45Fe3 and P45Fe5 were 511 ± 121 and 526 ± 110 MPa, which increased to 997±184 and 1003±193 MPa for P45B5Fe3 and P45B5Fe5 glass formulations, respectively. Table 6 shows the Weibull distribution of the tensile strength of the fibres investigated. It was observed that the trend of normalising fracture stress (σ_o) was consistent with the trend of average tensile strength. The Weibull modulus of these fibres was seen to range from 7.1 to 10.2.

The tensile modulus of the fibres showed the same profiles as the tensile strength. The difference in tensile modulus values for glass fibres with increasing Fe_2O_3 content were not seen to be statistically significant ($P > 0.05$). Whereas, the tensile modulus increased from 51.0±3 and 52.6±3 GPa to 62.1±4 to 63.7 ±4 GPa as 5 mol% B_2O_3 was added to the P45Fe3 and F45Fe5 glass systems, respectively.

DISCUSSION

Thermal Analysis

The thermal stability of the glasses in terms of processing window was found to increase with increasing B_2O_3 content (Figure 2). The processing window increased by 7% and 11% as 5 mol% B_2O_3 was added to the P45Fe3 and P45Fe5 glass systems, respectively. The reduction in the number of non-bridging oxygens was also suggested to be responsible for raising the temperature of the onset of crystallisation [26], which will eventually increase the processing window of the glasses. Harada *et al.* suggested that the addition of B_2O_3 suppressed the formation of orthophosphate Q^0 units, which promoted crystallisation [13]. They also suggested that addition of B_2O_3 could supress surface crystallisation due to the formation of highly cross-linked structure based on metaphosphate Q^2 tetrahedra. Therefore, it is suggested that addition of B_2O_3 to the phosphate glass network could alter the structure dimensionality of the phosphate network via the formation of chain-like Q^2 species rather

than Q^0 or Q^1 units, which in turn improved the processing window of the glasses as seen in Figure 2.

Fourier transforms infrared (FTIR) spectroscopy

The IR spectra (see Figure 3) showed the structural changes of the iron phosphate glasses due to B_2O_3 addition. When B_2O_3 is added to iron phosphate glasses, both P-O-B and P-O-Fe bonds will exist in the glass [27]. The bands observed at 729 cm^{-1} and 908 cm^{-1} in the IR spectra of the base iron phosphate glasses were assigned to symmetric and asymmetric stretching of P-O-P bridging bonds, respectively [28]. The band at 1245 cm^{-1} is assigned to the asymmetric vibrations of the non-bridging oxygen atoms in the phosphate chains.

With the addition of B_2O_3 the band at 1245 cm^{-1} became broader and the intensity reduced; this decrease in intensity reflects a reduction in the number of non-bridging P-O bonds and was indication of a progressive increase in the connectivity [29]. In borate glasses, the region around 850-1200 cm^{-1} was attributed to the B-O stretching of BO_4 units [30]. Therefore, it was likely that this connectivity was due to the replacement of P-O-P bonds with P-O-B links. The broadening of the bands in the region of 908 cm^{-1} also suggested formation of P-O-B bands as B_2O_3 was added. Both bands for asymmetric and symmetric stretching of P-O-P bridging oxygens shift to higher frequency as B_2O_3 was substituted for Na_2O. The absorption band near 1098 cm^{-1} have been assigned to $P\text{-}O^-$ groups (chain terminators) [31]. The $P\text{-}O^-$ absorption bands near 1098 cm^{-1} shifts to lower frequency as B_2O_3 replaces Na_2O. Similar shift for $P\text{-}O^-$ absorption bands to lower frequency was also observed by Bartholomew *et al.* for silver metaphosphate glasses [31]. They attributed such shift to the existence of covalent bonds between silver ions and the non-bridging oxygen.

Viscosity/ temperature

The viscosity/temperature plot was found to shift to higher temperature as B_2O_3 was added to the P45Fe3 and P45Fe5 glass forming liquids (see Figure 4). In general, the viscosity η is affected by the bonding energy between the cations and oxygens in the glass structure [32]. Therefore, the shift of viscosity/temperature plot to higher temperature region was expected as the structure of the glass forming liquids became strongly bonded when Na_2O was replaced by B_2O_3. Toyoda *et al.* studied the viscosity behaviour of several binary glass systems ($50RO\text{-}50P_2O_5$;R=Sr, Ca, Zn and Mg) and reported that the viscosity/ temperature curve shifted to higher temperature in the order of Ba<Sr<Ca<Mg which was similar to the order of

field strength of the respective ions [33]. They suggested that the structural rigidity of the glass structure increased with increasing cationic field strength which in turns increased the temperature/viscosity curve to higher temperature. A study of alkaline earth zinc phosphate glasses in the series of 20MO-30ZnO-50P_2O_5 (M=Br, Sr, Ca, Mg) by Striepe and Deubener also confirmed the effect of increasing field strength on the shift of viscosity / temperature curve to higher temperature [34]. They found that the fragility index *m* decreased with increasing field strength of the cations. The activation energy of viscous flow, which is an indication of energy required to sever sufficient bonds within the glass network to initiate flow [35], is strongly affected by the cross-linking [36] and chain length [37]. Sharifah *et al.* studied the effect of phosphate chain length on the activation energy of the viscous flow and reported that glass formulations with shorter chain lengths showed lower activation energy for viscous flow and vice versa [37]. Gray and Klein reported that the viscosity of phosphate glasses increased with increasing crosslinking [36]. Therefore, the shift of the viscosity/temperature plot to higher temperature with addition of B_2O_3 could be attributed to the fact that addition of boron to the phosphate glass network increased the cross-linking density and chain lengths by becoming or forming part of the glass network as also evidenced by the higher T_g and enhanced processing window.

The glass forming liquids can be characterised as strong or fragile based on the fragility index in which strong liquids exhibits low m values near T_g in the fragility plot and vice versa for the fragile liquids. The fragility is dependent on glass network polymerisation, which is highly altered by the addition of different modifying oxides [33]. The kinetic fragility parameter, *m* and $F_{1/2}$ estimated from the viscosity curve were found to decrease with the addition of B_2O_3. The decreasing value of fragility is an indication that the glass network is transforming from a fragile to strong network with the addition of B_2O_3. Richardson *et al.* studied the viscosity properties of sodium borophosphate glasses in the system of (1-x)$NaPO_3$-x$Na_2B_4O_7$ and found that the kinetic fragility parameter decreased with increasing sodium borate content [35]. They suggested that the decreasing fragility with increasing sodium borate content was due to the progressive depolymerisation of the phosphate network by the four coordinated boron atoms present in the glass network. The constant fragility may indicate that the coordination environment as well as the M-O-P bonds (where M = modifying oxides) in the glass network was not significantly altered [38]. However, the addition of Fe_2O_3 and/or FeO resulted in an increase in the fragility index. This result was attributed to a highly depolymerised structure, hence shorter chain lengths due to the higher

amount of Na_2O [39] and Fe_2O_3 [40]. Therefore, the decrease in the fragility values with the addition of B_2O_3 was an indication of longer phosphate chain length, which was also cross-linked by B^{3+} ions.

Fibre manufacturing

Glass formulations containing 5 mol% B_2O_3 (P45B5Fe3) were found to be considerably easier to fiberise than the only Fe_2O_3 and/or FeO (P45Fe3 and P45Fe5) containing glasses. However, glass formulations containing 5 mol% B_2O_3 with Fe_2O_3 and/or FeO contents fixed at 3 mol% (P45B5Fe3) were found to be qualitatively easier to fiberise than the glass formulations with 5 mol% B_2O_3 and 5 mol% Fe_2O_3 (P45B5Fe5). In this study, it was found that addition of 5 mol% B_2O_3 allowed for fibre manufacture from glass formulations with P_2O_5 content fixed at 45 mol% and this fibre production was continuous with no breakage for up to 3 hours. It was difficult to draw continuous fibres from the P45B5Fe5 glass formulation as the glass viscosity of this melt was close to the maximum temperature limit for the in-house melt-drawn fibre production system used.

The viscosity and average chain length of glass plays a very important role on the successful fibre drawing as it is difficult to pull continuous fibre from glass formulations with low viscosity and short average chain lengths [41]. Ahmed *et al.* investigated fibre manufacture of glass fibres from glasses with formulations fixed with 45, 50 and 55 mol% P_2O_5 and reported that it was possible to obtain fibres from the 50 and 55 mol% P_2O_5 compositions; however fibre manufacture from glasses with fixed 45 mol% P_2O_5 proved to be unsuccessful, which was attributed to the low viscosity and short average chain length of the glass compositions. It was observed that at high temperature the viscosity of the glasses was too low to pull fibre and upon lowering the temperature to achieve a suitable viscosity the glass was found to crystallise in the bushing of the crucible [41]. In our study it was possible to pull fibre from glass formulations with P_2O_5 content fixed to 45 mol%. It has been reported that, it is difficult to pull fibre from glass formulation with no B_2O_3, whereas addition of only 5 mol% B_2O_3 to the glass formulations made the fibre pulling comparatively easier and more importantly, continuous [15]. The MAS NMR analysis conducted on the glasses investigated in a study revealed that addition of 5 and 10 mol% B_2O_3 to the glass formulations with P_2O_5 content fixed to 40, 45 and 50 mol% increased the chain length [42]. PBG formulations with P_2O_5 content fixed at 45 mol% were contained shorter chains due to a mixture of Q^2 and Q^1 species (with the Q^1 and Q^2 ratios reportedly to be in the range of ~21 and ~81, respectively).

Whereas, formulations where P_2O_5 content was fixed at 45 mol% and B_2O_3 content fixed to 5 mol% reportedly had a longer chain structure composed mostly of Q^2 species (Q^1 and Q^2 ratios were reported to be in the range of ~8 and ~ 92, respectively). Therefore, it was assumed that the addition of B_2O_3 to the PBG formulations increased the chain length, which made the fibre pulling process continuous. Saranti *et al.* also suggested that addition of boron could alter the structure of the phosphate network via the formation of long chain Q^2 species rather than Q^0 or Q^1 units [1]. Successful fiberisation largely depends on the chain length and proper adjustment of melt temperature to obtain a suitable viscosity, since it is not feasible to draw fibres from glasses with low melt viscosities using the current approach. Sharifah *et al.* suggested that the decrease in fragility index corresponded to an increase in phosphate chain length and higher cationic field strength. Therefore, it is suggested that an increase in the chain length (i.e. Q^2 species) due to addition of B_2O_3 helped to ease manufacture of fibres from phosphate glass formulations with fixed P_2O_5 contents of 45mol% which was also evidenced by the decrease in fragility index as discussed above.

Initial mechanical properties of the fibres

The glass series investigated exhibited a trend of increasing fibre strength with the addition of B_2O_3 to the glass systems (see Figure 6). The tensile strength was found to have increased by 49% and 48% via addition of 5 mol% B_2O_3 to P45Fe3 and P45Fe5 glass formulations, respectively. The highest tensile strength (1003±193 MPa) was observed for P45B5Fe5 fibres. It has been reported that the tensile strength of P45B0 ($45P_2O_5$-16CaO-24MgO-$15Na_2O$) and P45B5 ($45P_2O_5$-16CaO-24MgO-$10Na_2O$-$5B_2O_3$) fibres are 530±67 MPa and 1050±96 MPa, respectively [15]. Therefore, there was no significant difference in the mechanical properties between P45Fe3, P45Fe5 and P45B0 fibres. Moreover, the mechanical properties of P45B5Fe3 and P45B5Fe5 fibres were also not significantly different from P45B5 fibres. Therefore, it could be concluded that the addition of Fe_2O_3 and/or FeO to the PBG formulations did not impart any significant effect on the mechanical properties of the fibres.

Ahmed *et al.* studied the mechanical properties of fibres drawn from $50P_2O_5$-40CaO-$5Na_2O$-$5Fe_2O_3$ glass and reported the tensile strength and modulus to be 456 MPa and 51.5 GPa, respectively [43]. The values obtained by Ahmed *et al.* compared well with the values obtained for the P45Fe3 and P45Fe5 formulations from this study. Felfel *et al*. reported the average tensile strength and modulus of 40 P_2O_5-24 MgO-16 CaO-$16Na_2O$-4 Fe_2O_3 fibres to

be 318±46 MPa and 73±10 GPa, respectively by [44]. The tensile strength of the fibres observed by Ahmed *et al.* and Felfel *et al.* were significantly lower than the values obtained for B_2O_3 containing fibres in this study.

Replacing monovalent cation oxides with divalent or trivalent/divalent cation oxides has been shown to increase the cross-link density which eventually increased the mechanical properties (tensile fracture stress and tensile modulus) of the fibres [45]. Addition of B_2O_3 to the phosphate glass structure can form highly cross-linked BPO_4 units which are composed of interconnected BO_4 and PO_4 tetrahedral units [46, 47]. Moreover, the inclusion of a second network former to phosphate based glasses increased the tensile strength and elastic modulus owing to the strong interaction between chain structures and the formation of three-dimensional structures [48]. As B_2O_3 is a natural glass network former [49-51], along with cross-linking, the borate ions can also participate in the formation of chain structures i.e. become a part of the backbone of the glass network.

Therefore, the improvement in fibre tensile strength with addition of B_2O_3 could be attributed to the fact that addition of boron to the phosphate glass network increased the cross-linking density and chain lengths by becoming or forming part of the glass network as also evidenced by higher T_g and enhanced processing window studies highlighted above.

The Weibull modulus of the fibres studied in the present study was seen to range from 7.1 to 10.2. Karabulut *et al*. studied the tensile strength of a series of phosphate based glass fibres drawn via the melt drawn system [52]. They found Weibull modulus values in the range between 6 and 12. The Weibull modulus (m) is a well-known and accepted method to describe the physics of fibre failure [53]. If a value of m is large, then stresses even slightly below the normalising value σ_o would lead to a low probability of failure. However, a low Weibull modulus would also introduce uncertainty about the strength of the fibre [25].

The tensile modulus of the P45Fe3 and P45Fe5 fibres was found to increase by ~18 % and 17% as 5 mol% B_2O_3 was added to the glass formulations. Similar effect of increasing B_2O_3 on the tensile modulus of the fibres had also been discussed by Sharmin et al. [15]. The tensile modulus of a material is an intrinsic property and depends on the field strength of the cation and the packing density of the oxygen atoms [54] as the cations with higher field strength can interact strongly with the negatively charged phosphate anions and therefore hinder mutual rotations and displacements of the anions [48]. Therefore, the increased

interaction between the negatively charged phosphate anions and the cations is attributed to the increased tensile modulus values of B_2O_3 containing fibres.

There was no statistical difference in the mechanical properties between P45B5Fe3 and P45B5Fe5 fibres and it was easier to pull P45B5Fe3 and P45B5Fe5 fibres, as compared to P45Fe3 and P45Fe5 fibres. Moreover, the mechanical properties of P45B5Fe3 and P45B5Fe5 fibres were also significantly higher than P45Fe3 and P45Fe5 fibres.

SUMMARY

The current study revealed a systematic relationship between composition and physical properties of the glasses in the system of P_2O_5-CaO-Na_2O-MgO-Fe_2O_3-B_2O_3**.** Four phosphate based glass compositions in the system P_2O_5-CaO-Na_2O-MgO-Fe_2O_3-B_2O_3 were produced by replacing the Na_2O with B_2O_3, and the P_2O_5 content was fixed at 45 mol%. The thermal stability of the glasses was also increased as 5 mol% B_2O_3 was added. The thermal expansion coefficient values, density and dissolution rate decreased with increasing B_2O_3. The viscosity was found to shift to higher temperature with increasing B_2O_3 content. The fragility parameter, *m* and $F_{1/2}$, estimated from the viscosity curve, decreases with B_2O_3 addition. The improved physical properties of the glasses investigated with B_2O_3 addition were attributed to the replacement of P-O-P bonds with P-O-B bonds. The presence of P-O-B bonds in the glass structure was confirmed by the FTIR analysis. Addition of B_2O_3 to the glass system enabled successful drawing of continuous fibres from glasses containing 3 and 5 mol% Fe_2O_3 with phosphate (P_2O_5) content fixed to 45 mol%. Moreover, the B_2O_3 containing fibres showed higher mechanical properties as compared to non-B_2O_3 containing ones. P45B5Fe5 fibres provided the highest tensile strength (1003±193 MPa).

REFERENCES

[1] Saranti A, Koutselas I, Karakassides MA. Bioactive glasses in the system $CaO–B_2O_3–P_2O_5$: Preparation, structural study and in vitro evaluation. Journal of Non-Crystalline Solids 2006;352:390-8.

[2] Knowles JC. Phosphate based glasses for biomedical applications. Journal of Materials Chemistry 2003;13:2395-401.

[3] Ahmed I, Lewis M, Olsen I, Knowles JC. Phosphate glasses for tissue engineering: Part 1. Processing and characterisation of a ternary-based P2O5-CaO-Na2O glass system. Biomaterials 2004;25:491-9.

[4] Abou Neel EA, Pickup DM, Valappil SP, Newport RJ, Knowles JC. Bioactive functional materials: a perspective on phosphate-based glasses. Journal of Materials Chemistry 2009;19:690-701.

[5] Ahmed I, Shaharuddin SS, Sharmin N, Furniss D, Rudd C. Core/Clad Phosphate Glass Fibres Containing Iron and/or Titanium. Biomedical glasses2015.

[6] Schiewer E, Lutze W, Boatner LA, Sales BC. Characterization of Lead-Iron Phosphate Nuclear Waste Glasses. MRS Online Proceedings Library 1985;50:null-null.

[7] Bingham PA, Hand RJ. Vitrified metal finishing wastes: I. Composition, density and chemical durability. Journal of Hazardous Materials 2005;119:125-33.

[8] Bingham PA, Hand RJ, Forder SD, Lavaysierre A. Vitrified metal finishing wastes: II. Thermal and structural characterisation. Journal of Hazardous Materials 2005;122:129-38.

[9] Ahmed IC, C. A. Lewis, M. P. Olsen, I. Knowles, J. C. . Processing, characterisation and biocompatibility of iron-phosphate glass fibres for tissue engineering. Biomaterials 2004;25:3223-32.

[10] Han N, Ahmed I, Parsons AJ, Harper L, Scotchford CA, Scammell BE, et al. Influence of screw holes and gamma sterilization on properties of phosphate glass fiber-reinforced composite bone plates. Journal of biomaterials applications 2013;27:990-1002.

[11] Arstila H, Vedel E, Hupa L, Hupa M. Factors affecting crystallization of bioactive glasses. Journal of the European Ceramic Society 2007;27:1543-6.

[12] Pemberton JE, Latifzadeh L, Fletcher JP, Risbud SH. Raman spectroscopy of calcium phosphate glasses with varying calcium oxide modifier concentrations. Chemistry of Materials 1991;3:195-200.

[13] Harada T, In H, Takebe H, Morinaga K. Effect of B_2O_3 Addition on the Thermal Stability of Barium Phosphate Glasses for Optical Fiber Devices. Journal of the American Ceramic Society 2004;87:408-11.

[14] Sharmin N, Hasan MS, Parsons AJ, Furniss D, Scotchford CA, Ahmed I, et al. Effect of Boron Addition on the Thermal, Degradation, and Cytocompatibility Properties of Phosphate-Based Glasses. BioMed Research International 2013;2013:12.

[15] Sharmin N, Parsons AJ, Rudd CD, Ahmed I. Effect of boron oxide addition on fibre drawing, mechanical properties and dissolution behaviour of phosphate-based glass fibres with fixed 40, 45 and 50 mol% P2O5. Journal of biomaterials applications 2014.

[16] Sharmin N, Hasan MS, Parsons AJ, Rudd CD, Ahmed I. Cytocompatibility, mechanical and dissolution properties of high strength boron and iron oxide phosphate glass fibre reinforced bioresorbable composites. Journal of the Mechanical Behavior of Biomedical Materials 2016;59:41-56.

[17] Seddon A, Tikhomirov V, Rowe H, Furniss D. Temperature dependence of viscosity of Er³⁺-doped oxyfluoride glasses and nano-glass-ceramics. Journal of Materials Science: Materials in Electronics 2007;18:145-51.

[18] Gent AN. Theory of the parallel plate viscometer. British Journal of Applied Physics 1960;11:85-7.

[19] Parsons AJ, Sharmin N, Shaharuddin SIS, Marshall M. Viscosity profiles of phosphate glasses through combined quasi-static and bob-in-cup methods. Journal of Non-Crystalline Solids 2015;408:76-86.
[20] Fulcher GS. Analysis of recent measurements of the viscosity of glasses. Journal of the American Ceramic Society 1925;8:339-55.
[21] Richert R, Angell CA. Dynamics of glass-forming liquids. V. On the link between molecular dynamics and configurational entropy. The Journal of Chemical Physics 1998;108:9016-26.
[22] Angell CA. Structural instability and relaxation in liquid and glassy phases near the fragile liquid limit. Journal of Non-Crystalline Solids 1988;102:205-21.
[23] Martinez L-M, Angell, C. A. A thermodynamic connection to the fragility of glass-forming liquids. Nature 2001;410:663-7.
[24] Ahmed I, Parsons AJ, Palmer G, Knowles JC, Walker GS, Rudd CD. Weight loss, ion release and initial mechanical properties of a binary calcium phosphate glass fiber/PCL composite. Acta Biomaterialia 2008;4:1307-14.
[25] Hull D, Clyne TW. An Introduction to Composite Materials: Cambridge University Press; 1996.
[26] Massera J, Claireaux C, Lehtonen T, Tuominen J, Hupa L, Hupa M. Control of the thermal properties of slow bioresorbable glasses by boron addition. Journal of Non-Crystalline Solids 2011;357:3623-30.
[27] Karabulut M, Yuce B, Bozdogan O, Ertap H, Mammadov GM. Effect of boron addition on the structure and properties of iron phosphate glasses. Journal of Non-Crystalline Solids;357:1455-62.
[28] Metwalli E, Brow RK. Modifier effects on the properties and structures of aluminophosphate glasses. Journal of Non-Crystalline Solids 2001;289:113-22.
[29] Kim N-J, Im S-H, Kim D-H, Yoon D-K, Ryu B-K. Structure and properties of borophosphate glasses. Electron Mater Lett 2010;6:103-6.
[30] Agathopoulos S, Tulyaganov DU, Ventura JMG, Kannan S, Saranti A, Karakassides MA, et al. Structural analysis and devitrification of glasses based on the CaO–MgO–SiO2 system with B2O3, Na2O, CaF2 and P2O5 additives. Journal of Non-Crystalline Solids 2006;352:322-8.
[31] Bartholomew RF. Structure and properties of silver phosphate glasses — Infrared and visible spectra. Journal of Non-Crystalline Solids 1972;7:221-35.
[32] Fujino S, Hwang, C. and Morinaga, K. Density, surface tension, and viscosity of BaO-ZnO-P2O5 glass melts. Shigen-to-Sozai 2003;119:423-6.
[33] Toyoda S, Fujino S, Morinaga K. Density, viscosity and surface tension of 50RO–50P2O5 (R: Mg, Ca, Sr, Ba, and Zn) glass melts. Journal of Non-Crystalline Solids 2003;321:169-74.
[34] Striepe S, Deubener J. Viscosity and kinetic fragility of alkaline earth zinc phosphate glasses. Journal of Non-Crystalline Solids 2012;358:1480-5.
[35] Gaylord S, Tincher B, Petit L, Richardson K. Viscosity properties of sodium borophosphate glasses. Materials Research Bulletin 2009;44:1031-5.
[36] C. GPEKL. Viscous flow of sodium phosphate glasses from 10^1 to 10^{14} poise. Society of Glass Technology 1986;27:241-4.
[37] Shaharuddin SIS, Ahmed I, Furniss D, Parsons AJ, Rudd CD. Thermal properties, viscosities and densities of glasses. Glass Technology - European Journal of Glass Science and Technology Part A 2012;53:245-51.
[38] Fang X, Ray CS, Day DE. Glass transition and fragility of iron phosphate glasses.: II. Effect of mixed-alkali. Journal of Non-Crystalline Solids 2003;319:314-21.

[39] Griffith EJ, Callis CF. Structure and Properties of Condensed Phosphates. XV. Viscosity of Ultraphosphate Melts1. Journal of the American Chemical Society 1959;81:833-6.
[40] Bushra Al-Hasni GM. Structural investigation of iron phosphate glasses using molecular dynamics simulation. Journal of Non-Crystalline Solids 2010;337:2775-9.
[41] Ahmed I, Lewis M, Olsen I, Knowles JC. Phosphate glasses for tissue engineering: Part 2. Processing and characterisation of a ternary-based P2O5–CaO–Na2O glass fibre system. Biomaterials 2004;25:501-7.
[42] Sharmin N, Hasan MS, Rudd CD, Boyd D, Werner-Zwanziger U, Ahmed I, et al. Effect of boron oxide addition on the viscosity-temperature behaviour and structure of phosphate-based glasses. Journal of Biomedical Materials Research Part B: Applied Biomaterials 2016:n/a-n/a.
[43] Ahmed IC, P. S. Abou Neel, E. A. Parsons, A. J. Knowles, J. C. Rudd, C. D. Retention of mechanical properties and cytocompatibility of a phosphate-based glass fiber/polylactic acid composite. Journal of Biomedical Materials Research Part B: Applied Biomaterials 2009;89B:18-27.
[44] Felfel RM, Ahmed I, Parsons AJ, Haque P, Walker GS, Rudd CD. Investigation of crystallinity, molecular weight change, and mechanical properties of PLA/PBG bioresorbable composites as bone fracture fixation plates. Journal of biomaterials applications 2012;26:765-89.
[45] Kurkjian CR. Mechanical properties of phosphate glasses. Journal of Non-Crystalline Solids 2000:207-12.
[46] Nam-Jin Kim S-HI, Dong-Hwan Kim, Duck-Ki Yoon, and Bong-Ki Ryu1. Structure and Properties of Borophosphate Glasses
Electron Mater Lett 2010;6:103-6.
[47] Koudelka L, Mošner P. Borophosphate glasses of the ZnO–B2O3–P2O5 system. Materials Letters 2000;42:194-9.
[48] Pukh VP, Baikova LG, Kireenko MF, Tikhonova LV, Kazannikova TP, Sinani AB. Atomic structure and strength of inorganic glasses. Physics of the Solid State 2005;47:876-81.
[49] Qiu D, Guerry P, Ahmed I, Pickup DM, Carta D, Knowles JC, et al. A high-energy X-ray diffraction, 31P and 11B solid-state NMR study of the structure of aged sodium borophosphate glasses. Materials Chemistry and Physics 2008;111:455-62.
[50] Rinke MT, Eckert H. The mixed network former effect in glasses: solid state NMR and XPS structural studies of the glass system (Na2O)x(BPO4)1-x. Physical Chemistry Chemical Physics 2011;13:6552-65.
[51] Carta D, Qiu D, Guerry P, Ahmed I, Abou Neel EA, Knowles JC, et al. The effect of composition on the structure of sodium borophosphate glasses. Journal of Non-Crystalline Solids 2008;354:3671-7.
[52] Karabulut M, Melnik E, Stefan R, Marasinghe GK, Ray CS, Kurkjian CR, et al. Mechanical and structural properties of phosphate glasses. Journal of Non-Crystalline Solids 2001;288:8-17.
[53] Parsons AJ, Ahmed, I., Yang, J., Cozien-Cazuc, S., Rudd C.D. Heat-treatment of phosphate glass fibres and its effect on composite property retention. 16th International Conference on Composite Materials 2007.
[54] Baikova LG, Fedorov, Y.K., Tolstoi, M.N., Pukh, V.P., Tikhonova, L.V.,, Lunter SGaS, A.B. Structural strength of phosphate glasses. The
Soviet Journal of Glass Physics and Chemistry 1991;16:211-7.

List of Figures

List of Tables

Figure 1

Click here to download Figure Figure 1_revised.tif

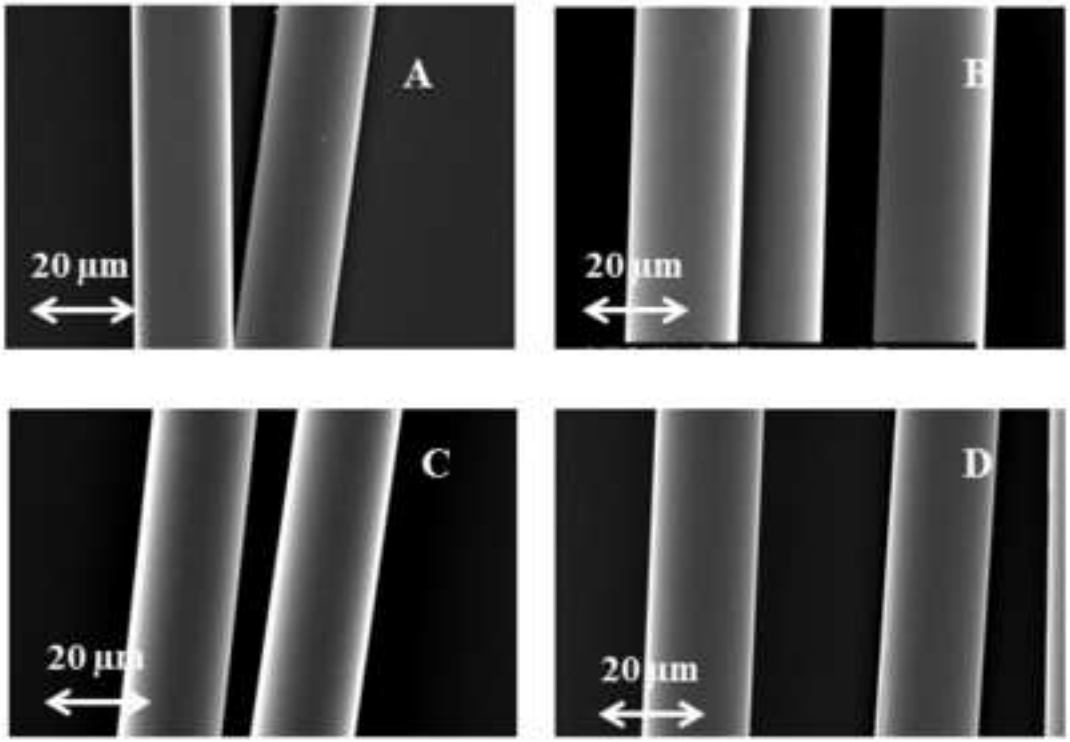

Figure 2

Click here to download Figure Figure 2.tif

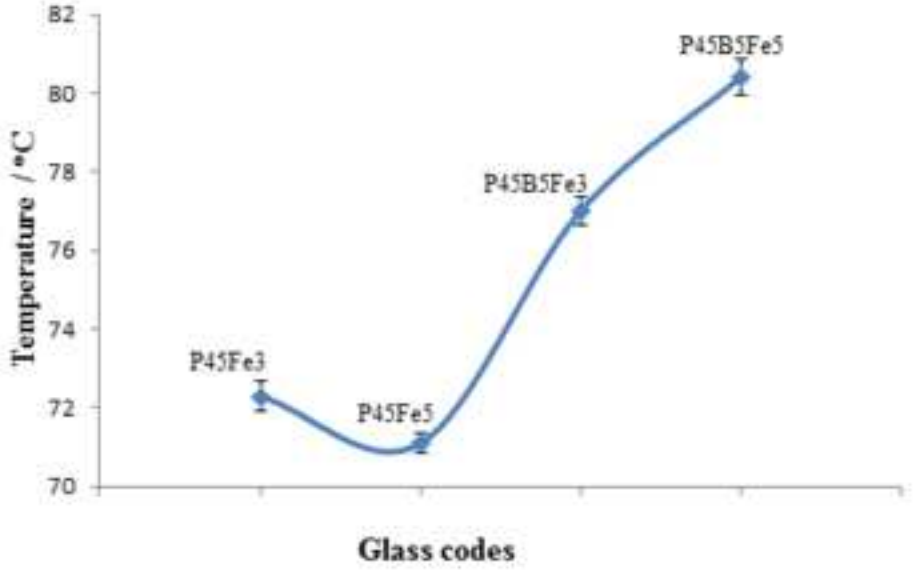

Figure 3

Click here to download Figure Figure 3.tif

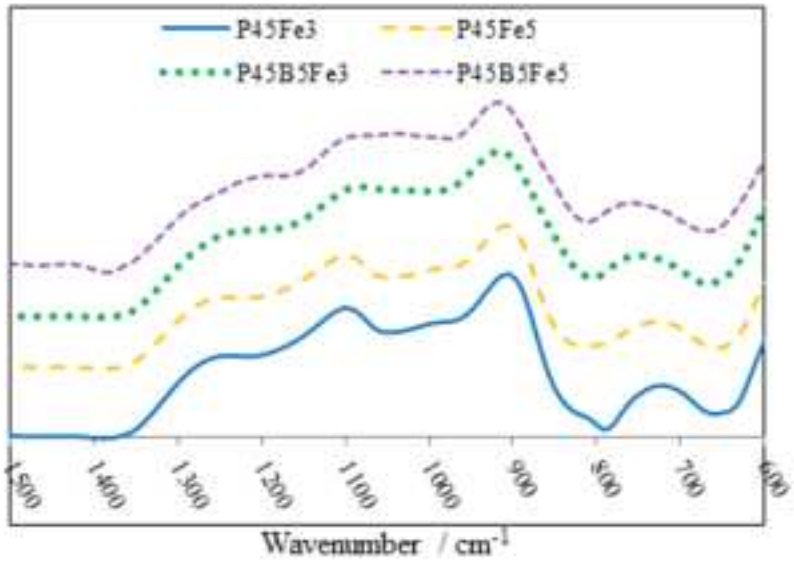

Figure 4

Click here to download Figure Figure 4.tif

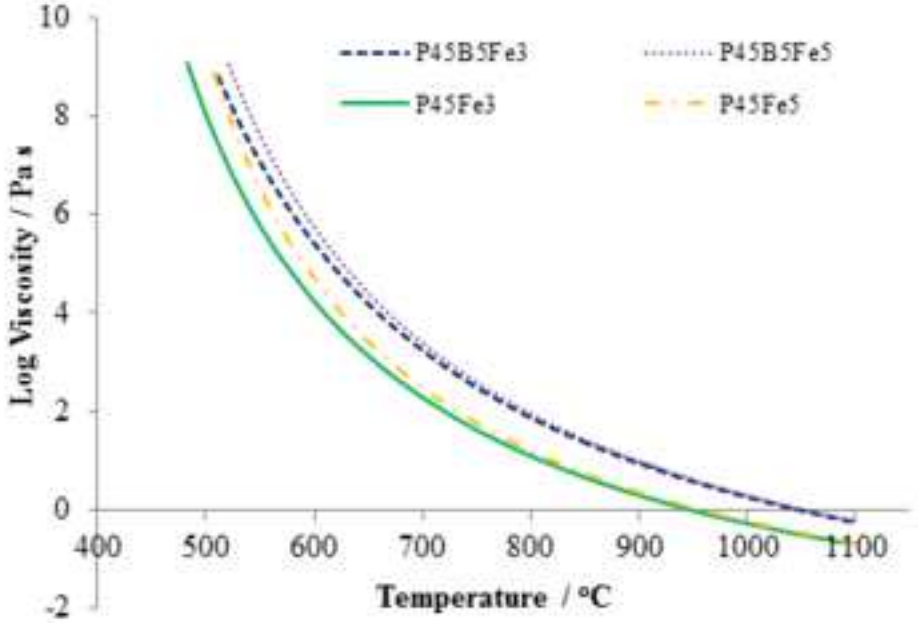

Figure 5

Click here to download Figure Figure 5.tif

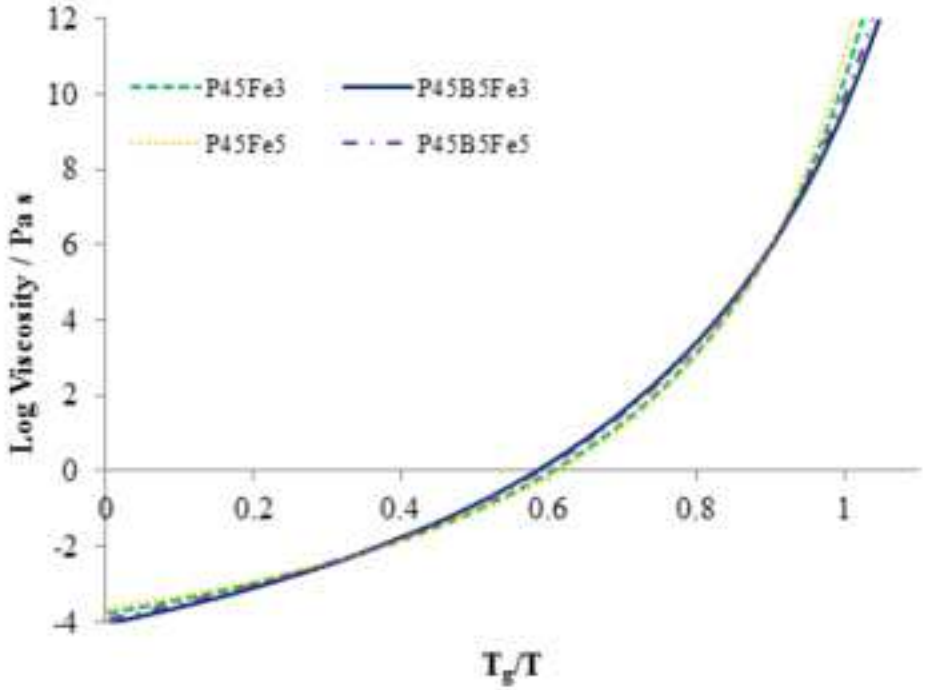

Figure 6

Click here to download Figure Figure 6.tif

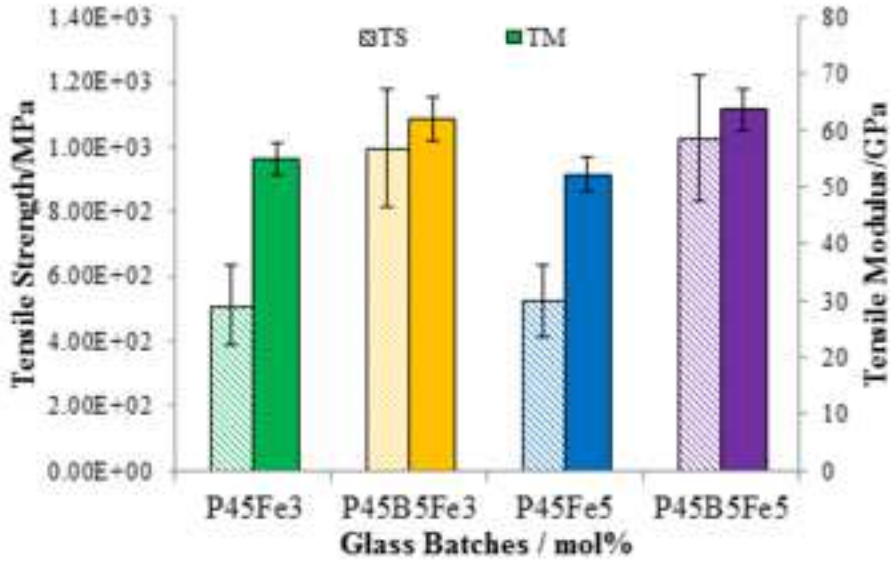

Table 1: *Glass batch compositions, drying, melting and casting temperature used throughout the study.*

Glass batch compositions / mol%	P_2O_5 Content / (mol%)	CaO Content / (mol%)	Na_2O Content / (mol%)	MgO Content / (mol%)	B_2O_3 Content / (mol%)	Fe_2O_3 Content / (mol%)	Dry Temp/ Time /(ºC/h)	Melt Temp/ Time /(ºC/h)	Casting Temp/ Time /(ºC/h)
P45Fe3	45	16	12	24	-	3	350/1	1150/1.5	450/1
P45Fe5	45	16	10	24	-	5	350/1	1150/1.5	456/1
P45B5Fe3	45	16	7	24	5	3	350/1	1150/1.5	484/1
P45B5Fe5	45	16	5	24	5	5	350/1	1150/1.5	510/1

Table 2: *Compositions of the glasses confirmed by ICP-AES*

Glass batch compositions/ mol%	P_2O_5 / mol%	CaO / mol%	Na_2O /mol%	MgO / mol%	B_2O_3 / mol%	Fe_2O_3 / mol%
P45Fe3	42.1 ± 0.3	15.4 ± 0.5	13.0 ± 0.3	26.9 ± 0.5	-	2.5 ± 0.1
P45Fe5	42.8 ± 0.4	15.4 ± 0.6	10.8 ± 0.5	26.8 ± 0.2	-	4.3 ± 0.1
P45B5Fe3	42.5 ± 0.3	15.6 ± 0.2	8.2 ± 0.1	27.1 ± 0.1	4.1 ± 0.1	2.4 ± 0.0
P45B5Fe5	42.1 ± 0.6	15.7 ± 0.2	6.5 ± 0.1	27.4 ± 0.3	4.2 ± 0.1	4.1 ± 0.1

Table 3: *The thermal characteristics (T_g, $T_{c,ons}$, T_c) for $45P_2O_5$-16CaO-24MgO-(12-x)Na_2O-3Fe_2O_3-xB_2O_3 and $45P_2O_5$-16CaO-24MgO-(10-x)Na_2O-5Fe_2O_3- xB_2O_3 (where x=0 and 5) glass systems.*

Glass batches / mol%	**T_g / °C**	**$T_{c,ons}$/ °C**
P45Fe3	470± 1.41	542± 0.5
P45Fe5	485 ± 1.9	553 ± 1
P45B5Fe3	502 ± 0.5	580 ± 1
P45B5Fe5	513 ± 1.0	593 ± 1

Table 4: *VFT equation constants for the glasses in the systems of* $45P_2O_5$*-16CaO-24MgO-(12-x)*Na_2O*-3*Fe_2O_3*-* xB_2O_3 *and* $45P_2O_5$*-16CaO-24MgO-(10-x)*Na_2O*-5*Fe_2O_3*-* xB_2O_3 *(where x=0 and 5).*

Glass batches / mol%	***A***	***B***	T_o
P45Fe3	-3.78	2493	289.1
P45Fe5	-3.65	2315	322.7
P45B5Fe3	-4.06	3180	264.1
P45B5Fe5	-3.94	3005	289.7

Table 5: *Fragility index values ($F_{1/2}$ and m) obtained for the glasses in the systems of $45P_2O_5$-16CaO-24MgO-(12-x)Na_2O-$3Fe_2O_3$-xB_2O_3 and $45P_2O_5$-16CaO-24MgO-(10-x)Na_2O-$5Fe_2O_3$- xB_2O_3 (where x=0 and 5).*

Glass batches / mol%	**$F_{1/2}$ (Eq.5)**	**m (Eq.4)**
P45Fe3	0.63	37
P45Fe5	0.64	45
P45B5Fe3	0.60	29
P45B5Fe5	0.61	32

Table 6: *Weibull distribution of fibres in the glass system of $45P_2O_5$-16CaO-24MgO-(12-x)Na_2O-3Fe_2O_3-xB_2O_3 and $45P_2O_5$-16CaO-24MgO-(10-x)Na_2O-5Fe_2O_3- xB_2O_3 (where x=0 and 5). The tensile fracture stress values are also included for the ease of comparison.*

Glass batches / mol%	**Tensile strength/MPa**	**Normalising fracture stress σ_o / MPa**	**Weibull modulus *m***
P45Fe3	511±121	540	8.1
P45Fe5	526±110	556	7.1
P45B5Fe3	997±184	1040	10.2
P45B5Fe5	1003±193	1054	7.9